Nuclear Engineering and Technology 52 (2020) 1537–1544

Contents lists available at ScienceDirect

Nuclear Engineering and Technology

journal homepage: www.elsevier.com/locate/net

Original Article

Primary damage of 10 keV Ga PKA in bulk GaN material under different temperatures

Huan He, Chaohui He*, Jiahui Zhang, Wenlong Liao, Hang Zang, Yonghong Li, Wenbo Liu**

School of Nuclear Science and Technology, Xi'an Jiaotong University, Xi'an, Shaanxi 710049, China

ARTICLE INFO

Article history:
Received 3 August 2019
Received in revised form
13 December 2019
Accepted 29 December 2019
Available online 30 December 2019

Keywords:
Molecular dynamics
Gallium nitride
Primary damage
Defects
Temperature

ABSTRACT

Molecular dynamics (MD) simulations were conducted to investigate the temperature effects on the primary damage in gallium nitride (GaN) material. Five temperatures ranging from 300 K to 900 K were studied for 10 keV Ga primary knock-on atom (PKA) with inject direction of [0001]. The results of MD simulations showed that threshold displacement energy (E_d) was affected by temperatures and at higher temperature, it was larger. The evolutions of defects under various temperatures were similar. However, the higher temperature was found to increase the peak number, peak time, final time and recombination efficiency while decreasing the final number. With regard to clusters, isolated point defects and little clusters were common clusters and the fraction of point defects increased with temperature for vacancy clusters, whereas it did not appear in the interstitial clusters. Finally, at each temperature, the number of Ga interstitial atoms was larger than that of N and besides that, there were other different results of specific types of split interstitial atoms.

1. Introduction

As a direct-bandgap semiconductor, GaN is commonly applied in optoelectronic and microelectronic devices. Compared with other semiconductors, such as silicon (Si) and silicon carbide (SiC), GaN has a larger direct band gap (3.4 eV) and higher electron mobility (2000 $cm^2/V \cdot s$). Because of its low sensitivity to ionizing radiation, it is a promising material for satellites and spacecrafts [1]. However, protons, α-particles, heavy ions and other particles which produce radiation effects in materials or devices widely exist in the whole space environment. There are three main radiation effects in semiconductor devices: single event effect, total dose effect, and displacement damage effect. Displacement damage, hard to recover, can severely influence the electrical properties and cause performance degradation in semiconductor devices. For designing and the reinforcement of devices, it is necessary to understand and assess the displacement damage in GaN material.

Studies on the displacement damage in GaN have been performed experimentally for several decades. Karmarkar et al. [2] reported a phenomenon that, due to high nonionizing energy loss (NIEL) of protons, 1.0 MeV protons could cause greater degradation than 1.8 MeV protons in GaN Schottky diodes. They also reported that annealing could help the recovery of displacement damage. Khanal et al. [3] carried out some experiments exposed to the 100 keV protons with different fluences and performance degradation was observed with increasing fluences.

Although some modern experimental facilities can observe or identify certain defects in semiconductors, such as transmission electron microscopy (TEM), deep level transient spectroscopy (DLTS), whereas, they have some limitations on observing the whole irradiation process. However, computer simulations are good tools to understanding the displacement damage in semiconductor devices. Compared with experiments, the simulations about the displacement damage in GaN were relatively fewer and most of them were discussing the defect properties by *ab-initio* calculations [4–6] or directly focusing on the devices by finite element methods [7]. Whereas, displacement damage is a multi-scale problem which spans from the primary damage at the atomic-level and 10^{-15} s to electrical properties at the device-level and 10^6 s.

MD simulations were applied commonly in some studies to accurately describe primary damage in materials. However, there were a few researches about the primary damage in GaN. Nord et al. [8] proposed an empirical potential of GaN. It is an analytical bond-order potential which provides a good fit to some critical properties

* Corresponding author.
** Corresponding author.
E-mail addresses: hechaohui@xjtu.edu.cn (C. He), liuwenbo@xjtu.edu.cn (W. Liu).

https://doi.org/10.1016/j.net.2019.12.027

including defects of GaN. Based on this potential, they reported that most of the damage was isolated point defects or small clusters for the recoils between 200 eV and 10 keV [9] and they also found that under the same radiation condition, GaN was less damaged compared with Si. Besides the recoil atoms, swift heavy ions were also used in some simulations. Ullah et al. [10] investigated the optical properties under F, P, and PF4 irradiation by experiments and simulations. They found that the lighter ions were easier to produce isolated point defects and the number of defects produced by PF4 was similar to the sum of one P and four F ions separately. In recent development of potentials for primary damage simulations [11–13], previous classical potentials had some limitations on simulating accurately in high energy as they lacked enough short-range interactions. Thus, Ziegler-Biersack-Littmark (ZBL) screened potential which gives a good representation of the short-range interactions is required to connect with them. Based on the work of Nord et al. [8], an improved potential [12] was put forth to solve this problem. In their studies, they presented the details about how to obtain the hybrid potential and they also studied defects and clusters for energies ranging from 500 eV to 40 keV. Their results showed that NIEL in GaN was smaller than the classic model.

However, there are still some problems less understanding, especially the relationship of temperature with primary damage is not yet known. Thus, this study mainly discusses this factor and the results will be helpful in the researches of multi-scale modeling of displacement damage and future researches.

2. Methods

Primary damage in GaN was performed by, Large-scale Atomic/Molecular Massively Parallel Simulation (LAMMPS) [14]. This code has been widely used in modeling the primary damage of materials including metals [15,16] and semiconductors [17–19]. In MD simulations, atomic interactions among atoms, which are often defined as interatomic potentials, should be carefully applied due to their essential influence to simulation results. The potential was introduced from the work of Nord et al. [8] and Chen et al. [12]. What is more, the electronic effect was not considered in this research.

At ambient temperature and pressure, GaN always presents a wurtzite crystal structure. The simulation cell was created based on an orthogonal unit cell which was converted from two hexagonal unit cells. Primary damage was always modeled by providing kinetic energy to a specific atom, which is defined as PKA. In this study, Ga PKA was only considered because the damage of Ga is more severe than N at same energy due to its heavy mass. Ga with 10 keV kinetic energy was chosen from the top-center of the simulation cell. $50 \times 50 \times 50$ unit cells which contain 1 million atoms were established in a simulation box to prevent PKA from moving out. Thermostat region which controls the temperature on five sides except the top side was 8 Å in length and periodic boundary conditions were applied on all sides [17–19]. The simulation model was shown in Fig. 1(a).

Since semiconductor devices always work at room temperature and the maximum operated temperature of GaN material was reported to be about 1000 K [1]. Five different temperatures, 300 K, 450 K, 600 K, 750 K, and 900 K, were applied in this study. It also was reported that the inject direction of PKA truly affects the evolution of primary damage in UO_2 [20] and $LiAlO_2$ [21]. Therefore, the inject directions of PKA in the present simulations are mainly around [0001] which is a high symmetry direction. Thirty different random directions with a little angle around [0001] direction were used to obtain statistical results. PKA directions were illustrated in Fig. 1(b) and the little angle is added to avoid the channeling effect. Multiple-phase timestep procedure which was applied successfully in the researches of primary damage of 3C–SiC [17,18] were also adopted. The time step varies from 10^{-5} to 10^{-3} ps and the total time from PKA excitation to the end is 12.4 ps.

Six types of point defects, i.e., vacancies (V_{Ga} and V_N), interstitial atoms (I_{Ga} and I_N) and antisite atoms (Ga_N and N_{Ga}), were investigated. Defects were defined by Wigner-Seitz cell method [22] which is constructed by the Voronoi method. An empty site is a vacancy whereas a site with two more atoms corresponds to an interstitial atom. Since there are few sites containing three or more atoms in a lattice site, two atoms in a site were only considered in this study. In addition, the antisite atom is identified with the comparison of previous atom type and the present one. As far as clusters, defects within the cutoff distance which is one and a half times lattice constant (3.186 Å) [10] in GaN are regarded as a cluster and the number of defects contained in a cluster refers to the size of clusters.

3. Results and discussion

3.1. Threshold displacement energy of Ga

E_d, which plays a significant role in the primary damage calculations, is often applied in some damage related models, such as Norgett, Robison, and Torrens (NRT) equation [23] or arc-dpa models [24]. There are several definitions about E_d depending on the situation [25]. In our simulations, E_d of Ga was defined as the lowest energy of PKA Ga which causes permanent displacement off the initial lattice site at a certain direction. Since E_d is a statistical value which is averaged by enough directions, the following approximations were adopted to obtain more accurate results. The system of 2304 atoms was applied for modeling E_d and binary search algorithm was conducted to determine the final energy. 1) One designated Ga atom in the center of the system was chosen as the PKA. 2) Azimuthal angles and polar angles were chosen randomly in each simulation. 3) the total time of 8.2 ps was chosen to avoid the recombination of defects.

Though more simulation times mean more accurate results, a proper choice to reduce computing resource is significant. In a recent research [26] about calculation of E_d of UO_2, 100 simulations were enough to obtain a converged result with a reasonable certainty. Therefore, a test to determine how the mean value was affected by the number of simulations was carried out. In order to obtain a more accurate conclusion, the number of simulations was extended to 5000 at 750 K and the result was shown in Fig. 2. It can be suggested that even though increase the number of simulations, the mean value would not be affected a lot (less than 1 eV) after 1000 simulations. And this phenomenon indicated that 1000 simulations are enough to obtain an accurate result of E_d of Ga.

Consequently, 1000 times were simulated at each temperature. The statistical results were shown in Fig. 3 and their error bars referred to the standard error of the mean (SEM), which is the standard deviation divided by the size of the sample. Although the mean value of 750 K seems slightly lower than that of 600 K, it can be clearly seen that temperature indeed affects the value of E_d overall and the values of E_d are significantly larger for higher temperatures, especially comparing values of 300 K with that of 900 K. In addition, the results under different temperatures are close to the value which is 45eV obtained by previous reports [9]. Compared this value with some other semiconductors [27–29], E_d of Ga is the largest one among β-SiC(C~40eV, Si~60eV), Si(~36eV) and GaAs(Gã13eV, As~13eV). This provides a possible explanation that GaN has a greater resistance to displacement damage than other semiconductors.

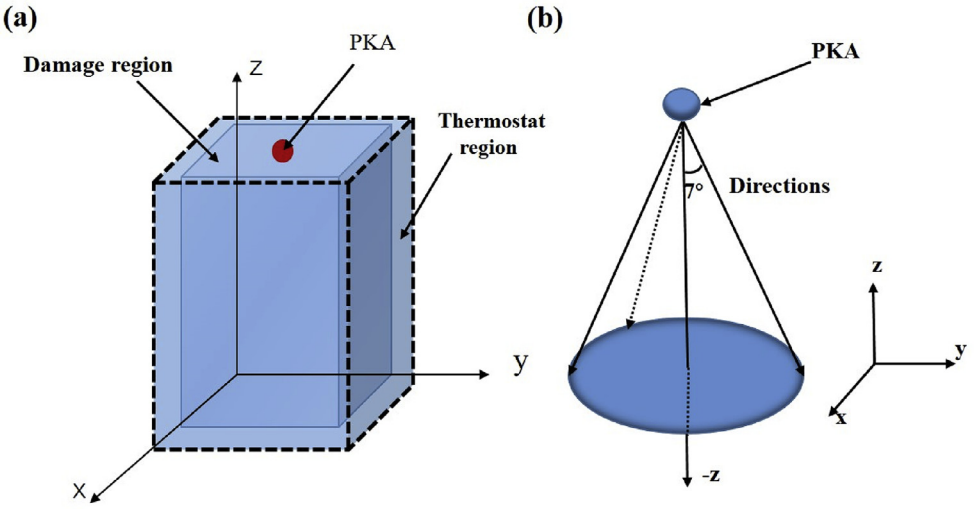

Fig. 1. Schematic diagram of (a) the simulation model (b) PKA directions.

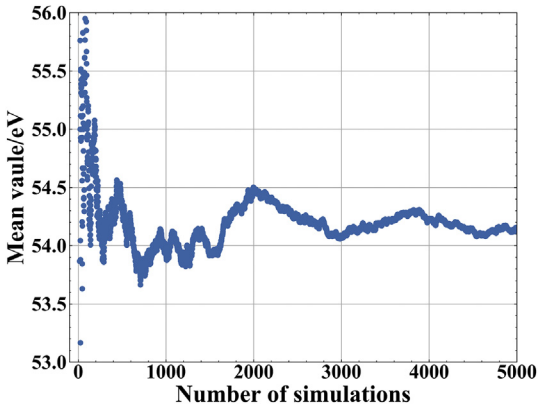

Fig. 2. The mean value of E_d of Ga as a function of the number of simulations at 750 K

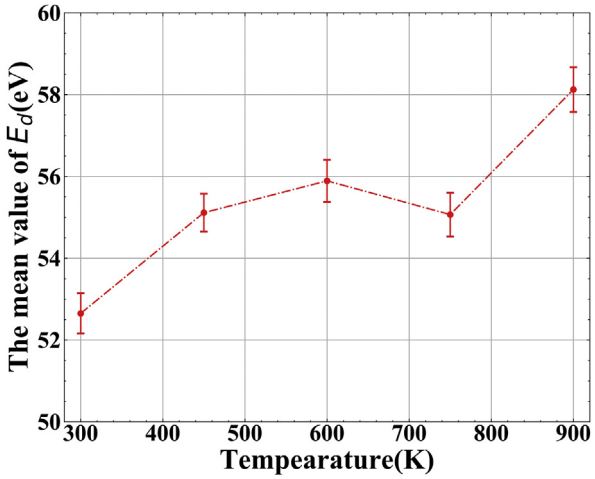

Fig. 3. The mean value of E_d of Ga under different temperature (the error bars indicate the SEM).

3.2. Production of defects

There are two main stages in the collision by timescale. In the first stage, defects are always produced and increase a lot during a rapid time (~0.1 ps) induced by an energetic particle. The energetic particle dissipates its most energy (more than 90%) by colliding with atoms and thus displaces nearby atoms from their original sites to form defects. While, in the subsequent stage (~1–10 ps) which is often called a heat spike stage, the number of defects decreases. The reason is that vacancies and interstitial atoms within certain distance spontaneously recombine with each other and some other defect recombination reactions. Consequently, the maximum number of defects always occurs at the end of the first stage.

In order to get a better understanding of the primary damage in GaN, Wigner-Seitz cell method was applied to distinguish defects from normal atoms. Positions of different types of defects at four typical time points were shown in one case at 300 K in Fig. 4. It can be clearly seen that the number of defects increases rapidly within 0.4 ps and then decreases relatively slowly. Furthermore, most defects tend to aggregate together in the whole process and they seem to gather in the upper part which nears the position of PKA.

However, these snaps are too simple to understand the whole processes clearly. To quantitatively evaluate the evolutions of the number of defects in primary damage, plenty of time points was chosen to obtain enough data under different temperatures. During the whole primary damage, vacancies and interstitial atoms tend to form Frenkel pairs which is a common type of defect appeared in the irradiated crystal. Owing to this fact, the number of vacancies is equal to interstitial atoms. Therefore, the number of Frenkel pairs was used to represent the number of vacancies or interstitial atoms.

Results of the evolution of average number of Frenkel pairs and antisite atoms were respectively shown in Fig. 5. It can be clearly seen that the evolution trends of Frenkel pairs and antisite atoms are similar under different temperatures. Specifically, from the beginning to peak time, where it is about 0.5 ps, a number of defects are produced and the number of defects increases continuously. Following the peak time, the number of defects decreases slowly due to the recombination and it keeps at a stable value after about 7 ps in the end. Compared with the process of production, the rate of recombination is a little lower. This evolution has a good agreement with classic theory and previously reported simulations [12,15,17,18]. However, a similar evolution does not represent the

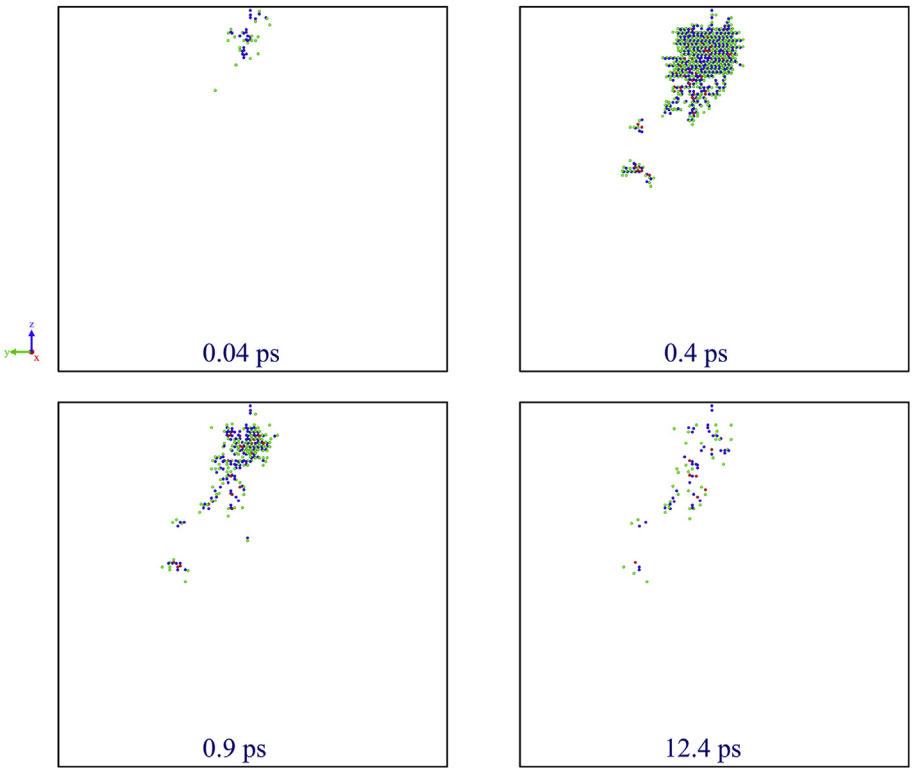

Fig. 4. Snaps of distribution of all defects for 10 keV Ga PKA at 300 K.
(Blue atoms are vacancy, green atoms are interstitial atoms and red atoms are antisite atoms).

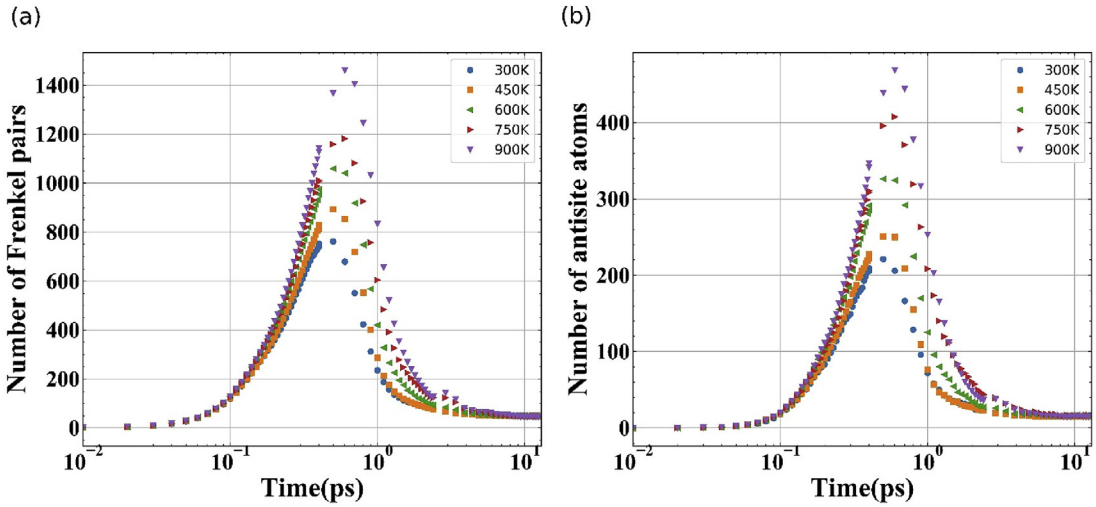

Fig. 5. Evolutions of average number of (a) Frenkel pairs and (b) antisite atoms under different temperatures.

same phenomenon. It is clearly seen that at a higher temperature, the peak number of Frenkel pairs and antisite atoms are both higher. Hence, the specific properties of Frenkel pairs were concentrated in the following discussions.

During the whole primary damage, there are two attractive time points, peak time and final time. Peak time refers to the time of maximum number of defects. However, there are no accurate definitions about final time because the number of defects fluctuates around a value at the end of heat spike stage. Due to the criterion of Wigner-Seitz method, therefore, if the standard deviation of number of defects of a time point with its afterwards values is less than 1, this time point was within the end of heat spike stage. And the minimum time point was chosen as the value of final time. As for recombination efficiency, it is defined as follows:

$$\varphi = \frac{N_{peak} - N_{final}}{N_{peak}} \quad (1)$$

Where N_{peak} is the peak number of defects and N_{final} is the final number of defects. The peak number is the maximum number of

Table 1
Parameters about Frenkel pairs under different temperatures (the errors refer to the standard error of mean).

Temperature/K	Peak number	Peak time/ps	Final number	Final time/ps	Recombine efficiency/%
300	798.37 ± 62.44	0.44 ± 0.01	51.30 ± 1.15	9.83 ± 0.44	92.48 ± 0.55
450	935.87 ± 98.08	0.48 ± 0.02	48.50 ± 1.01	10.03 ± 0.42	93.51 ± 0.53
600	1105.53 ± 115.87	0.50 ± 0.02	46.73 ± 1.20	10.52 ± 0.33	94.63 ± 0.45
750	1261.37 ± 148.96	0.52 ± 0.20	46.70 ± 1.74	10.53 ± 0.36	95.07 ± 0.46
900	1528.17 ± 157.95	0.58 ± 0.02	45.70 ± 0.82	11.20 ± 0.22	96.06 ± 0.38

defects produced in the whole process and the final number refers to the last number of defects. Detailed parameters were shown in Table 1. All of the parameters in Table 1 are averaged parameters from thirty simulations at a specific temperature.

Based on the data in Table 1, it can be inferred that temperature indeed affects the properties of Frenkel pairs. With temperature increasing, the peak number increases greatly. The reason is that at higher temperature, the vibration of each atom is larger than at low temperature region, which could weaken the bonding state of Ga–N, and thus easily displace these atoms, especially at the ballistic stage. In contrast, the final number of defects decreases a little with temperature, which is due to the higher recombination rate at high temperature. In addition, all of the recombination efficiencies are larger than 90%. As for the peak time, the influence of temperature is not clear, where the time is about 0.4–0.6 ps. However, there is a large discrepancy in the final time, from 9.8 ps to 11.2 ps. This discrepancy confirms that higher temperature could delay the final time obviously in the primary damage. The reason is probably more defects are produced at peak time at a higher temperature so that it needs more time to recombine and reach the final stage.

Based on previous calculations of E_d under different temperatures, our results were also compared with NRT equation and another work [9] by J. Nord et al., in which the final number was 46.7 for 10 keV Ga PKA. NRT equation has been a standard model to predict the final number of Frenkel pairs in the researches of radiation effects for several decades. Its formula was shown as below:

$$N_d = \frac{0.8E_{PKA}}{2E_d} \tag{2}$$

Where the N_d corresponds to the final number of Frenkel pairs and the value E_d is adopted by previous calculations. The comparisons were illustrated in Fig. 6.

It can be seen that our results are similar as the value in J.Nord's work and the trend of NRT equation is also similar as our results.

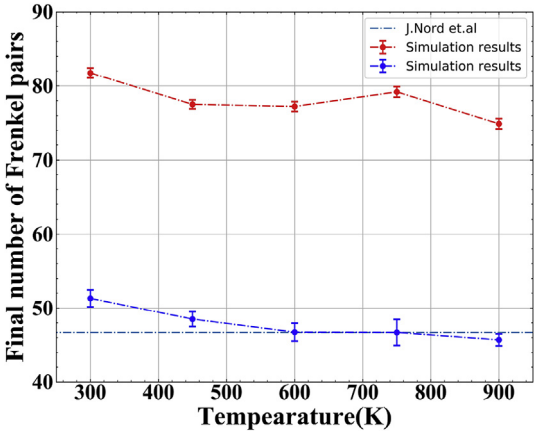

Fig. 6. Final number of Frenkel pairs of our simulation, NRT equation. and data from this work [9] under different temperatures (the error bars indicate the SEM).

Therefore, it can be assumed that the difference of final number of Frenkel pairs under different temperatures probably is caused by the E_d. However, it can be seen that NRT equation overestimates the final number of Frenkel pairs compared to another two results.

3.3. Defect clusters

In the primary damage, there are not only isolated point defects, but also clusters. Cluster also plays an important role in the material mechanical and electrical properties, such as swelling behavior and carrier migration.

By using the cluster analysis method presented in Section.2, the cluster sizes and their numbers under different temperature were shown in Fig. 7. The results indicated that the cluster size is independent on irradiation temperatures. And in the primary damage of GaN, isolated point defects and little clusters (size < 5) are more likely to appear. This feature which enhances the damage recombination probability was reported in this study [9]. However, there are some differences between the clusters of vacancy and interstitial atom. As for large clusters, it can be clearly seen that the sizes of vacancy clusters are larger than that of interstitial atom clusters. For instance, at 450 K, there are even some vacancy clusters' sizes larger than 15. Some other materials [30,31] were also reported the similar results. Based on a model of temperature and clusters [32], since interstitials and vacancies may be both mobile during this temperature range, the formation of clusters are complex to cause this phenomenon.

Since point defects are the most common defect in the primary damage, the fraction of point defects in their corresponding clusters under different temperatures were shown in Fig. 8. As for vacancy clusters, the fraction was larger as temperature increases, from 66.8% to 72.3%. This phenomenon indicated that vacancy cluster may be thermally unstable so that there are more isolated vacancies at a higher temperature. Nevertheless, this trend did not appear in the interstitial clusters and interstitial clusters may be thermally stable.

3.4. Split interstitial atoms

Interstitial atoms have interesting properties compared with other point defects, especially in the binary material. Their high mobility rate makes them possible to move long distance, even at low temperature, and form different types of interstitial atoms, such as split, octahedral or tetrahedral interstitial atoms. Owing to the limitations of Wigner-Seitz defect analysis method, it can only identify the interstitial atoms as the split interstitial atoms. Therefore, a new perspective was presented here to investigate the configurations of interstitial atoms further in molecular dynamics, especially for the binary compound.

Based on our assumptions, there are two main types of split interstitial atoms divided by the type of foreign interstitial atoms, Ga and N interstitial atoms. Furthermore, for different original lattice sites, we divided each into three types. The schematic diagram was illustrated in Fig. 9. Take Ga interstitial atoms for instance, there are two common interstitial atoms, Ga–N (Ga) and

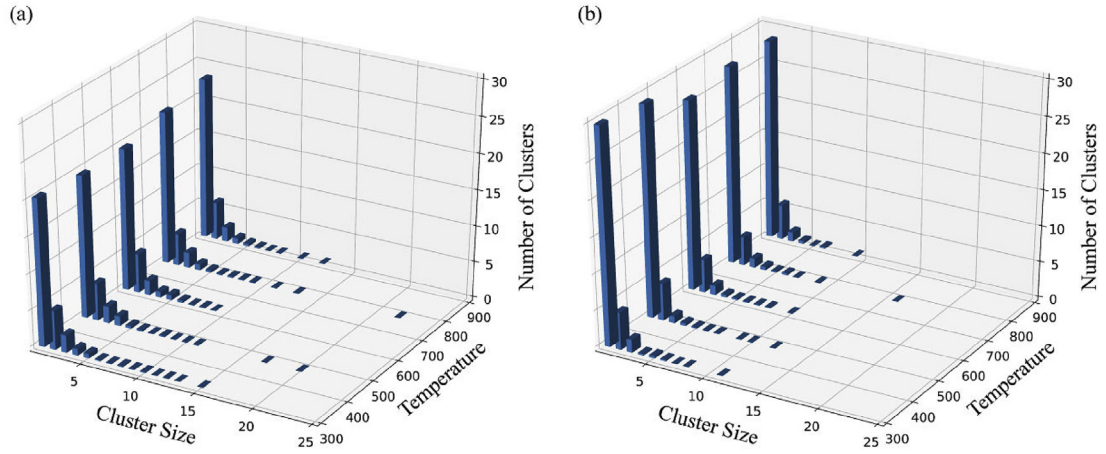

Fig. 7. Cluster sizes and their numbers under different temperatures.
(a) vacancy clusters, (b) interstitial atom clusters

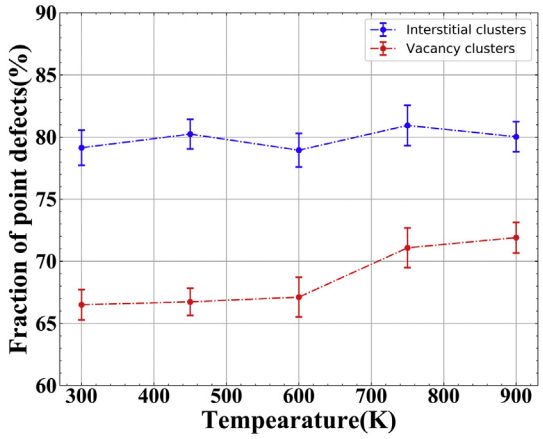

Fig. 8. Fraction of point defects under different temperatures (the error bars indicate the SEM).

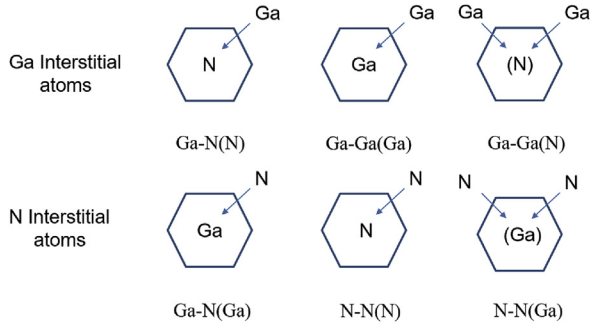

Fig. 9. Schematic diagram of different split interstitial atoms.

Ga–Ga (Ga) (the element in the bracket corresponds to the original atom in lattice site) and one special interstitial atoms Ga–Ga (N).

By comparing the original type and the present type of atoms, the number of six types of split interstitial atoms under different temperatures were shown in Table 2.

Though there are no correlations of split interstitial atoms with temperatures from this table, some other attracting properties of them are founded at each temperature. Firstly, the number of Ga interstitial atoms is larger than N interstitial atoms. The main reason may be the difference of E_d of these two atoms. In our and previous reported calculations [4,9], E_d of Ga atoms is far less than N atoms. This property mainly causes Ga atoms are easier to displace from their original lattice sites even produce defects than N atoms. In addition, it can be seen that Ga–Ga (N) and N–N (Ga) are very difficult to form, especially Ga–Ga (N). It may be determined by the mechanisms of them that these two types of defects need to knock out the original atoms in a lattice site before forming them, while the energy to knock out atoms may be a little large.

Meanwhile, the number of Ga–N (N) (18.56) is founded a bit larger than that of Ga–Ga (Ga) (7.21) whereas the number of Ga–N (Ga) (8.56) is a little less than that of N–N (N) (9.37). It is an opposite result for themselves, since for Ga interstitial atoms, the hetero-atomic pair (Ga–N (N)) is easier to form than homo-atomic pair (Ga–Ga (Ga)) however N interstitial atoms are in contrast. In the previous studies of formation energy, some calculations [4,9] reported the split-interstitial atoms in GaN. The results of Xiao et al. [4] showed the formation energy of four types of split interstitial atoms at Ga and N sites along the <11$\bar{2}$0> direction under N-rich conditions. For Ga interstitial atoms, the formation energy of Ga–Ga(Ga) is 12.34 eV, a bit larger than 10.99 of Ga–N(N). While for N interstitial atoms, the formation energy of N–N(N) is 4.57 eV, a little less than 4.61eV of Ga–N(Ga). The difference and its relative value of formation energy agree well with that of the specific number, whatever Ga or N interstitial atoms, though this method surely has some deficiencies on identifying the more sophisticated types.

4. Conclusions

MD simulations were carried out to investigate the primary damage caused by 10 keV Ga PKA under five different temperatures along [0001] directions. The effects of temperature on several properties, including E_d, production of defects, clusters and split interstitial atoms are given.

Based on the analysis, all the properties studied were affected by temperature, but not all showed a clear trend. E_d is determined by temperature and at higher temperature, it becomes larger. The effect of temperature on E_d may further affect the final number of point defects at various temperatures. Under different temperatures, the evolutions of defects are similar. However, higher temperature increases the peak number largely and decreases the final

Table 2
Number of different types of split interstitial atoms under different temperatures, (Ga Int means the total number of Ga interstitial atoms, N Int as well).

Temperature/K	Ga–N(N)	Ga–Ga(Ga)	Ga–Ga(N)	Ga Int	Ga–N(Ga)	N–N(N)	N–N(Ga)	N Int
300	20.30	6.80	0.00	27.10	10.07	10.17	2.43	22.67
450	19.23	8.00	0.03	27.26	8.37	9.30	2.23	19.90
600	17.57	6.77	0.07	24.41	8.63	8.87	2.77	20.27
750	17.40	7.43	0.10	24.93	7.83	9.80	2.67	20.30
900	18.30	7.07	0.07	25.44	7.90	8.73	2.30	18.93
Mean Value	18.56	7.21	0.05	25.83	8.56	9.37	2.48	20.41

number slightly. As a result, the recombination efficiency is larger at a higher temperature. Temperature has little effects on the peak time while delays final time evidently. It is due to larger amount of defects is produced at peak time which needs more time to reach the steady state. Our results were also compared with NRT equation and another work. It consistent well with the value in their work and the trend of NRT equation. It is assumed that the final number of Frenkel pairs is affected by the change of E_d under different temperatures and the NRT equation overestimates this value. As for clusters, isolated point defects and little clusters are commonly produced and vacancy are easier to form large clusters than interstitial atoms.

Temperature could increase the fraction of isolated vacancy in vacancy clusters, because vacancy cluster may be thermally unstable. And this phenomenon does not reflect in the interstitial clusters. Finally, for interstitial atoms, the number of Ga is always larger than N. The reason is that E_d of Ga is less than that of N. Ga–Ga (N) and N–N (Ga) are very difficult to form due to the formation mechanisms of them. In addition, there is also an interesting point that the number of Ga–N (N) is larger than that of Ga–Ga (Ga) whereas the number of Ga–N (Ga) is larger than that of N–N (N). This is probably caused by the value of their formation energy.

Declaration of competing interest

The authors declared that they have no conflicts of interest to this work. We declare that we do not have any commercial or associative interest that represents a conflict of interest in connection with the work submitted.

Acknowledgements

The research was supported by Science Challenge Project (No. TZ2018004), National Natural Science Foundation of China (No. 11575138, 11835006, 11690040, 11690043, 11705137) and NSAF Joint Fund (No. U1830124). We would like to acknowledge the “H2” High Performance Cluster.

Appendix A. Supplementary data

Supplementary data to this article can be found online at https://doi.org/10.1016/j.net.2019.12.027.

References

[1] S. Pearton, GaN and ZnO-Based Materials and Devices, Springer Science & Business Media, 2012.
[2] A.P. Karmarkar, B.D. White, D. Buttari, D.M. Fleetwood, R.D. Schrimpf, R.A. Weller, L.J. Brillson, U.K. Mishra, Proton-induced damage in gallium nitride-based Schottky diodes, IEEE Trans. Nucl. Sci. 52 (2005) 2239–2244, https://doi.org/10.1109/TNS.2005.860668.
[3] M.P. Khanal, S. Uprety, V. Mirkhani, S. Wang, K. Yapabandara, E. Hassani, T. Isaacs-Smith, A.C. Ahyi, M.J. Bozack, T.-S. Oh, M. Park, Impact of 100 keV proton irradiation on electronic and optical properties of AlGaN/GaN high electron mobility transistors (HEMTs), J. Appl. Phys. 124 (2018) 215702, https://doi.org/10.1063/1.5054034.
[4] H.Y. Xiao, F. Gao, X.T. Zu, W.J. Weber, Threshold displacement energy in GaN: ab initio molecular dynamics study, J. Appl. Phys. 105 (2009) 123527, https://doi.org/10.1063/1.3153277.
[5] H.Y. Xiao, X.T. Zu, F. Gao, W.J. Weber, Ab initio calculations of structural and energetic properties of defects in gallium nitride, J. Appl. Phys. 103 (2008) 123529, https://doi.org/10.1063/1.2947604.
[6] C.G. Van de Walle, J. Neugebauer, First-principles calculations for defects and impurities: applications to III-nitrides, J. Appl. Phys. 95 (2004) 3851–3879, https://doi.org/10.1063/1.1682673.
[7] M. Zerarka, P. Austin, A. Bensoussan, F. Morancho, A. Durier, TCAD simulation of the single event effects in normally-OFF GaN transistors after heavy ion radiation, IEEE Trans. Nucl. Sci. 64 (2017) 2242–2249, https://doi.org/10.1109/TNS.2017.2710629.
[8] J. Nord, K. Albe, P. Erhart, K. Nordlund, Modelling of compound semiconductors: analytical bond-order potential for gallium, nitrogen and gallium nitride, J. Phys. Condens. Matter 15 (2003) 5649, https://doi.org/10.1088/0953-8984/15/32/324.
[9] J. Nord, K. Nordlund, J. Keinonen, Molecular dynamics study of damage accumulation in GaN during ion beam irradiation, Phys. Rev. B 68 (2003) 184104, https://doi.org/10.1103/PhysRevB.68.184104.
[10] M.W. Ullah, A. Kuronen, K. Nordlund, F. Djurabekova, P.A. Karaseov, K.V. Karabeshkin, A.I. Titov, Effects of defect clustering on optical properties of GaN by single and molecular ion irradiation, J. Appl. Phys. 114 (2013) 183511, https://doi.org/10.1063/1.4829904.
[11] J. Byggmästar, F. Granberg, K. Nordlund, Effects of the short-range repulsive potential on cascade damage in iron, J. Nucl. Mater. 508 (2018) 530–539, https://doi.org/10.1016/j.jnucmat.2018.06.005.
[12] N. Chen, E. Rasch, D. Huang, E.R. Heller, F. Gao, Atomic-scale simulation for pseudometallic defect-generation kinetics and effective NIEL in GaN, IEEE Trans. Nucl. Sci. 65 (2018) 1108–1118, https://doi.org/10.1109/TNS.2018.2822243.
[13] R.E. Stoller, A. Tamm, L.K. Béland, G.D. Samolyuk, G.M. Stocks, A. Caro, L.V. Slipchenko, Y.N. Osetsky, A. Aabloo, M. Klintenberg, Y. Wang, Impact of short-range forces on defect production from high-energy collisions, J. Chem. Theory Comput. 12 (2016) 2871–2879, https://doi.org/10.1021/acs.jctc.5b01194.
[14] S. Plimpton, Fast Parallel algorithms for short-range molecular dynamics, J. Comput. Phys. 117 (1995) 1–19, https://doi.org/10.1006/jcph.1995.1039.
[15] S. Qurat-ul-ain, K. Yong-Soo, Primary radiation damage characterization of α-iron under irradiation temperature for various PKA energies, Mater. Res. Express 5 (2018), 046518, https://doi.org/10.1088/2053-1591/aabb6f.
[16] M.J. Rahman, M.W.D. Cooper, B. Szpunar, J.A. Szpunar, Primary radiation damage on displacement cascades in UO_2, ThO_2 and $(U_{0.5}Th_{0.5})O_2$, Comput. Mater. Sci. 154 (2018) 508–516, https://doi.org/10.1016/j.commatsci.2018.08.024.
[17] D.E. Farrell, N. Bernstein, W.K. Liu, Thermal effects in 10 keV Si PKA cascades in 3C–SiC, J. Nucl. Mater. 385 (2009) 572–581, https://doi.org/10.1016/j.jnucmat.2009.01.036.
[18] J.Q. Xi, P. Zhang, C. H He, M. J Zheng, H. Zang, D.X. Guo, L. Ma, Evolution of defects and defect clusters in β-SiC irradiated at high temperature, Fusion Sci. Technol. 66 (1) (2014) 235–244, https://doi.org/10.13182/FST13-740.
[19] C. Liu, I. Szlufarska, Distribution of defect clusters in the primary damage of ion irradiated 3C-SiC, J. Nucl. Mater. 509 (2018) 392–400, https://doi.org/10.1016/j.jnucmat.2018.07.010.
[20] L. Van Brutzel, J.-M. Delaye, D. Ghaleb, M. Rarivomanantsoa, Molecular dynamics studies of displacement cascades in the uranium dioxide matrix, Philos. Mag. 83 (36) (2003) 4083–4410, https://doi.org/10.1080/14786430310001616081.
[21] H. Tsuchihira, T. Oda, S. Tanaka, Displacement cascade simulation of LiAlO2 using molecular dynamics, J. Nucl. Mater. 414 (1) (2011) 44–52, https://doi.org/10.1016/j.jnucmat.2011.04.064.
[22] S. Alexander, Visualization and analysis of atomistic simulation data with OVITO–the Open Visualization Tool, Model. Simul. Mater. Sci. Eng. 18 (2010), 015012, https://doi.org/10.1088/0965-0393/18/1/015012.
[23] M.J. Norgett, M.T. Robinson, I.M. Torrens, A proposed method of calculating displacement dose rates, Nucl. Eng. Des. 33 (1975) 50–54, https://doi.org/10.1016/0029-5493(75)90035-7.
[24] K. Nordlund, S.J. Zinkle, A.E. Sand, F. Granberg, R.S. Averback, R. Stoller, T. Suzudo, L. Malerba, F. Banhart, W.J. Weber, F. Willaime, S.L. Dudarev, D. Simeone, Improving atomic displacement and replacement calculations with physically realistic damage models, Nat. Commun. 9 (2018) 1084,

https://doi.org/10.1038/s41467-018-03415-5.
[25] K. Nordlund, J. Wallenius, L. Malerba, Molecular dynamics simulations of threshold displacement energies in Fe, Nucl. Instrum. Methods Phys. Res. Sect. B Beam Interact. Mater. Atoms 246 (2006) 322–332, https://doi.org/10.1016/j.nimb.2006.01.003.
[26] B. Dacus, B. Beeler, D. Schwen, Calculation of threshold displacement energies in UO_2, J. Nucl. Mater. (2019), https://doi.org/10.1016/j.jnucmat.2019.04.002.
[27] R. Devanathan, T. Diaz de la Rubia, W.J. Weber, Displacement threshold energies in β-SiC, J. Nucl. Mater. 253 (1998) 47–52, https://doi.org/10.1016/S0022-3115(97)00304-8.
[28] E. Holmström, A. Kuronen, K. Nordlund, Threshold defect production in silicon determined by density functional theory molecular dynamics simulations, Phys. Rev. B 78 (2008), 045202, https://doi.org/10.1103/PhysRevB.78.045202.
[29] N. Chen, S. Gray, E. Hernandez-Rivera, D. Huang, P.D. LeVan, F. Gao, Computational simulation of threshold displacement energies of GaAs, J. Mater. Res. 32 (8) (2017) 1555–1562, https://doi.org/10.1557/jmr.2017.46.
[30] C. Liu, I. Szlufarska, Distribution of defect clusters in the primary damage of ion irradiated 3C-SiC, J. Nucl. Mater. 509 (2018) 392–400, https://doi.org/10.1016/j.jnucmat.2018.07.010.
[31] Wei Yang, et al., Molecular dynamics simulations of displacement cascade and threshold energy in ordered alloy Al3U, Nucl. Instrum. Methods Phys. Res. Sect. B Beam Interact. Mater. Atoms 449 (2019) 22–28, https://doi.org/10.1016/j.nimb.2019.01.025.
[32] S.J. Zinkle, 1.03-Radiation-Induced effects on microstructure, Compr. Nucl. Mater. 1 (2012) 65–98.